# LANGMUIR

pH Reversible Encapsulation of Oppositely Charged Colloids Mediated by Polyelectrolytes

Yong Guo, [ID] Bas G. P. van Ravensteijn,[†][ID] Chris H. J. Evers, and Willem K. Kegel*

Van 't Hoff Laboratory for Physical and Colloid Chemistry, Debye Research Institute, Utrecht University, Paduálaan 8, 3584 CH Utrecht, The Netherlands

[S] Supporting Information

ABSTRACT: We report the first example of reversible encapsulation of micron-sized particles by oppositely charged submicron smaller colloids. The reversibility of this encapsulation process is regulated by pH-responsive poly(acrylic acid) (PAA) present in solution. The competitive adsorption between the small colloids and the poly(acrylic acid) on the surface of the large colloids plays a key role in the encapsulation behavior of the system. pH offers an experimental knob to tune the electrostatic interactions between the two oppositely charged particle species via regulation of the charge density of the poly(acrylic acid). This results in an increased surface coverage of the large colloids by the smaller colloids when decreasing pH. Furthermore, the poly(acrylic acid) also acts as a steric barrier limiting the strength of the attractive forces between the oppositely charged particle species, thereby enabling detachment of the smaller colloids. Finally, based on the pH tunability of the encapsulation behavior and the ability of the small colloids to detach, reversible encapsulation is achieved by cycling pH in the presence of the PAA polyelectrolytes. The role of polyelectrolytes revealed in this work provides a new and facile strategy to control heteroaggregation behavior between oppositely charged colloids, paving the way to prepare sophisticated hierarchical assemblies.
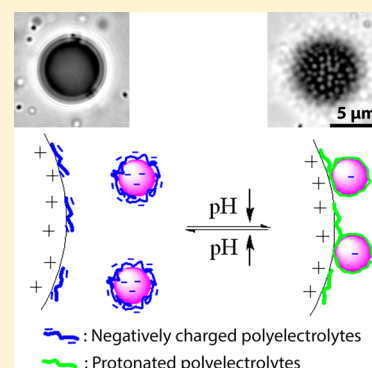
1. INTRODUCTION

Heteroaggregation is a clustering process that occurs between different species of particles and has proven to be a facile strategy for the preparation of a wide variety of (colloidal) clusters/assemblies.[1−4] The shape and structure of the formed clusters depend strongly on the size ratio and volume fractions of the participating particle species. Following this strategy a variety of superstructures have been prepared, including colloidal chains[4] and colloidal crystals.[2,3] A particularly interesting class of heteroaggregates are so-called raspberry-like composites. These clusters are formed when aggregation is induced between particles with vastly different dimensions(size ratio of $D_{large}/D_{small} > 3$, where D_{large} and D_{small} represent the diameters of large colloid and small colloid, respectively). The resulting cluster comprises a central large particle that is encapsulated by the smaller particles.[5,6] The morphology of these clusters is characterized by large surface areas and high surface roughness. Naturally, these parameters are set by the choice of the smaller encapsulation particles. Additionally, by using chemically modified smaller colloids, raspberry-like composites with controllable surface chemistry can be prepared. Owing to these key features, raspberry-like composites have great potential in applications such as catalyst immobilization platforms,[7−9] superhydrophobic films,[10,11] and sensors.[12,13] To optimize the performance of these rough particles, many efforts have been devoted to precisely control the formation process of raspberry-like composites by using a variety of heteroaggregation strategies. Commonly applied strategies include electro-statics,[14,15] azide−alkyne click reactions,[16] colloidal steric stabilization,[12,17] epoxy-amine reactions,[10,18] and noncovalent host−guest interactions.[1] Despite this variety of strategies, the majority of the resulting raspberry-like aggregates are formed irreversibly due to strong attractions compared to the thermal energy between the two particle species. An exception is the work of Yang et al.[1] who reported reversible raspberry-like composites by utilizing photoresponsive host−guest inter-actions to induce aggregation between the participating particle species. The disadvantage of their method is the requirement of extensive surface functionalization procedures.

Heteroaggregation is obviously not limited to synthetic (colloidal) constructs but is also frequently exploited in biological systems. For example, the heteroaggregation of negatively charged nucleic acids (DNA or RNA) and net positively charged proteins is for a large part responsible for the formation of virus capsids. In contrast to the synthetic strategies toward heteroaggregates mentioned above, the formation of virus capsids often is a fully reversible process. The reversibility is governed by a pH-responsive charge density of the individual capsid proteins due to the presence of acidic and basic moieties.[19−22]

Inspired by the reversibility of nucleic acid encapsulation displayed by many viruses, we set out to design a reversible

encapsulation system consisting of positively charged large polystyrene microspheres and negatively charged small polystyrene nanospheres that were decorated with a pH-responsive poly(acrylic acid) (PAA) polyelectrolyte outer layer. Because the charge density of the PAA-coated particles can be regulated by adjusting pH of the dispersion, we anticipated observing pH-dependent encapsulation. At high pH, where the immobilized PAA polyelectrolytes are deprotonated, the particles bear their maximum negative charge, which should result in a high tendency for heteroaggregation. By lowering pH, the surface charge of the PAA-coated particles decreases, which is expected to lead to disintegration of the hetero-aggregates. However, although we found a distinct pH-dependence on the encapsulation behavior, interestingly the trend we observed was completely opposite to our expectation. These initially unexpected results could be rationalized by taking into account the presence of very low concentrations of free PAA-rich polyelectrolytes in the continuous phase that had leached from the PAA-coated particles. By systematically investigating the influence of free PAA on the encapsulation behavior, we were able to identify an experimental window in which the electrostatic mediated encapsulation process was completely reversible.

2. EXPERIMENTAL SECTION

2.1. Materials. Styrene (St, 99%), divinylbenzene (DVB, 55% mixture of isomers, tech. grade), acrylic acid (AA, 99%), [2-(methacryloyloxy)ethyl]trimethylammonium chloride (METMAC, 80 wt % in H_2O), poly(acrylic acid) (PAA, M_w = 450 kg·mol^{-1}), polyvinylpyrrolidone (PVP, M_w = 40 kg·mol^{-1}), methanol, sodium chloride (NaCl), and sodium hydroxide (NaOH) were obtained from Sigma-Aldrich. Potassium persulfate (KPS, >99% for analysis) and azobis(isobutyronitrile) (AIBN, 98%) were purchased from Acros Organics. Hydrochloric acid (HCl, 36−38%, chem. pure) was obtained from Merck. All chemicals were used as received. The water used throughout all of the experiments was purified using a Milli-Q water purification system.

2.2. Synthesis of Positively Charged Large Polystyrene Microspheres (PLPS). PLPS were synthesized by stabilizer-free dispersion polymerization using METMAC as comonomer.[23,24] A 37.5 mL sample of methanol, 12.5 mL of H_2O, 10 mL of styrene, 91 mg of AIBN, and 123 μL of METMAC were added into a 100 mL three-necked round-bottom flask equipped with a condenser, mechanical stirrer, and nitrogen gas inlet. The monomer mixture was purged with nitrogen for 30 min. After degassing, the mixture was mechanically stirred and heated to 75 °C to initiate the polymerization. The reaction was allowed to proceed for 8 h under nitrogen atmosphere. The final product was centrifuged at 500*g* for 3 min and washed with ethanol and H_2O sequentially to remove unreacted reagents as well as secondary nuclei. Finally, the resulting particles were stored in H_2O.

2.3. Synthesis of Negatively Charged PAA-Decorated Small Polystyrene Nanospheres (CPSAA). CPSAA were synthesized by surfactant-free emulsion polymerization using acrylic acid as comonomer.[25] A 45 mL sample of H_2O, 5.5 mL of St, 381 μL of AA, and 27.5 μL of DVB were added into a 100 mL three-necked round-bottom flask, followed by 25 mg of KPS dissolved in 5 mL of H_2O. While being bubbled with nitrogen gas, the mixture was constantly stirred with a mechanical stirrer. After 15 min, the nitrogen inlet was raised above the liquid level for another 15 min. Subsequently, the flask was immersed in a 70 °C water bath to initiate the polymerization. The reaction was allowed to proceed for 24 h under nitrogen atmosphere. The final product was centrifuged at 15 000*g* for 15 min and washed with ethanol and H_2O sequentially to remove unreacted reagents. Finally, the obtained colloids were stored in H_2O.

2.4. Synthesis of Negatively Charged Small Polystyrene Nanospheres (CPS). CPS nanospheres were prepared using a similar method as described for CPSAA. The key difference was the absence of AA in the reaction mixture. A 45 mL sample of H_2O, 4.7 mL of St, and 140 μL of DVB were added into a 100 mL three-necked round-bottom flask, followed by 156 mg of KPS dissolved in 7.5 mL of H_2O. The flask was constantly stirred with a mechanical stirrer under nitrogen flow. Subsequently, the flask was immersed in a 80 °C water bath to initiate the polymerization. The reaction was allowed to proceed for 24 h under nitrogen atmosphere. The final product was centrifuged at 15 000*g* for 15 min and washed with ethanol and H_2O sequentially to remove unreacted reagents. Finally, the particles were stored in H_2O.

2.5. Encapsulation Process. For all experiments, the small colloids were added in large excess. The number ratio of small colloids over large colloids was approximately 18 000. Typical procedures to form clusters of oppositely charged colloids were as follows: 146 μL of 13.7 mM aqueous HCl solution and 4 μL of H_2O were added into a 1.5 mL conical centrifuge tube and mixed via shaking by hand. Subsequently, 5 μL of PLPS dispersion (solid content = 0.5 wt %) was added and mixed. Finally, 45 μL of CPSAA dispersion (solid content = 1 wt %) was added and homogenized by shaking. The final dispersion was immediately placed on a roller-table and left to equilibrate for 1 h. After this period, 5 μL of the dispersion was placed on a homemade microscopy cell (for details, see Characterization). The resulting aggregates were directly observed by optical microscopy. Exact quantities and variations on this standard procedure are listed in Table S1 of the Supporting Information.

To investigate the desorption of the smaller colloids and the reversibility of the encapsulation process, 13.7 mM aqueous NaOH solution was added to tune the pH to a desired value. After addition, the sample was equilibrated for 1 h before observation.

To investigate the influence of dissolved PAA on the surface coverage of the large positively charged particles by the smaller negatively charged colloids, commercial PAA was added to the particle dispersion during the heteroaggregation process. A final PAA concentration of 5 × 10^{-6} g·ml^{-1} was used. The samples were prepared following an analogous procedure as described before. First, PAA was dissolved in water followed by the addition of the negatively charged colloids. Lastly, the positively charged colloids were added.

2.6. Characterization. Transmission electron microscope (TEM) pictures were taken with a Philips Tecnai 10 electron microscope typically operating at 100 kV. The samples were prepared by drying a drop of diluted aqueous dispersion on top of polymer-coated copper grids.

Infrared (IR) spectra were obtained using a PerkinElmer Frontier FT-IR/FIR spectrometer. The attenuated total reflectance (ATR) mode was used. Measurements were carried out on powders obtained by drying the particle dispersion.

Optical microscopy (OM) images were taken with a Nikon Ti-E inverted microscope. The microscope was equipped with a Nikon TIRF NA 1.49 100× oil immersion objective, intermediate magnification of 1.5×, and a Hamamatsu ORCA Flash camera. The used microscopy cell was constructed as follows: all glass slides were cleaned with water, ethanol, and Kimtech precision wipes before use. Two coverslip glasses (VWR, #0, 22 × 22 mm) were placed at a distance of approximately 15 mm from each other on a microscope slide (Menzel-Gläser) and fixated using tape. Subsequently, a drop of dispersion was injected in between the coverslips. The sample cell was then closed by taping an additional coverslip (Menzel-Gläser, #1.5, 22 × 22 mm) on top of the two immobilized coverslips. The sample was monitored through the coverslip side of the sample cell.

The hydrodynamic diameters of the particles were measured using dynamic light scatting (DLS). Measurements were performed on a Malvern Zetasizer Nano instrument. Highly diluted, aqueous samples were prepared at various pH values. The total ionic strength was adjusted to 10 mM for all samples. The measurements were taken in 7 runs of 15 individual acquisitions at a scattering angle of 173°. The data was analyzed using the cumulant method.

Zeta potentials were determined by laser Doppler electrophoresis using the same instrument as used for DLS. Highly diluted, aqueous samples were prepared at various pH values. The total ionic strength

of these samples was equal to 1 mM. The radii of particles (R) were approximately 250 nm, while the Debye length (κ^{-1}) is on the order of 10 nm under the conditions at which the electrophoresis measurements were conducted. Hence, $\kappa R \gg 1$, justifying the use of the Smoluchowski limit of the Henry equation to convert the measured electrophoretic mobilites into the reported zeta potentials.[26]

3. RESULTS AND DISCUSSION

3.1. Synthesis of Particles PLPS, CPS, and CPSAA. Dispersion polymerization was chosen to synthesize PLPS because it allows for the preparation of particles in the micrometer size regime. The relatively large size of the resulting particles enables us to study the encapsulation behavior in situ by optical microscopy. METMAC was used as comonomer during the dispersion polymerization. The permanently charged quaternary amine functionality of the comonomer provides a highly hydrophilic character to this monomer, ensuring that the charged moieties will predominantly reside at the outer surface rather than in the hydrophobic interior of the formed colloids. The presence of positive charges also ensures colloidal stability of the particles. Figure 1a,b show an optical micrograph and
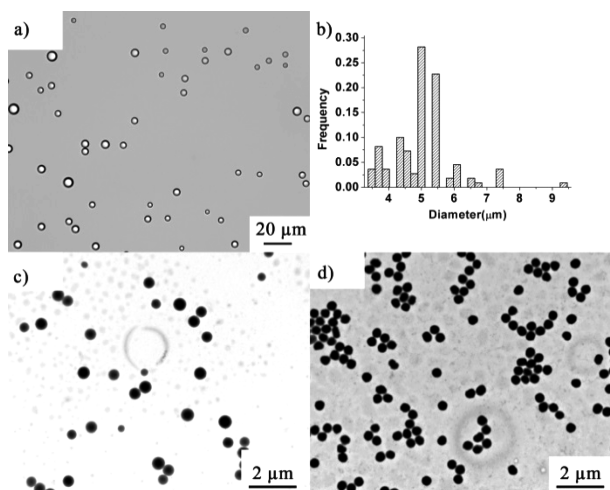
corresponding size distribution of the prepared PLPS, respectively. The size distribution was obtained by measuring 100 particles in several optical micrographs of as-synthesized PLPS. The PLPS had a broad size distribution with a diameter of 5 ± 1 μm. Because the smaller particles used for the encapsulation experiments are significantly smaller than even the smallest PLPS particles, curvature effects are expected to be absent and hence the polydispersity of PLPS has no influence on the encapsulation behavior. Electrophoretic mobility measurements revealed a highly positive zeta potential equal to 55.7 ± 8.2 mV, indicating successful incorporation of METMAC onto the particle surface.

To synthesize CPS, emulsion polymerization was used, being the method of choice to synthesize submicron, charge stabilized particles. The typical dimensions of colloids obtained using emulsion polymerization procedures guarantee that they are sufficiently large to be observed using optical microscopy, but small enough compared to PLPS. As mentioned before, this large size difference between PLPS and the smaller negatively charged colloids is key in ensuring efficient encapsulation. The emulsion polymerization was performed using KPS as radical initiator. Upon decomposition of KPS, negatively charged sulfate radicals initiate the polymerization. These charged moieties eventually reside at the particle surface generating the desired negatively charged particles. Figure 1c shows a typical TEM image of the obtained CPS colloids, revealing relatively monodisperse particles with a diameter of 460 ± 50 nm. DLS measurements showed a hydrodynamic diameter of 470 ± 18 nm. As anticipated, the particles were negatively charged as reflected by their zeta potential of −61.7 ± 7.0 mV.

CPSAA was synthesized following essentially the same emulsion polymerization procedure as employed for the preparation of CPS. The key difference was that during the CPSAA synthesis, acrylic acid (AA) was present as comonomer, resulting in particles decorated with a PAA-rich surface shell.[25] Figure 1d shows a representative TEM image of CPSAA which reveals monodisperse colloids with a diameter of 400 ± 15 nm. To confirm the incorporation of AA, infrared (IR) spectroscopy was used. Figure 2a shows IR spectra of CPS (bottom, red) and CPSAA (top, black). Evidently, compared to the spectrum obtained for CPS, the spectrum of CPSAA contains an additional signal at 1706 cm^{-1}. This vibration corresponds to the C=O stretching of the incorporated AA. Successful AA incorporation was further confirmed by measuring the zeta
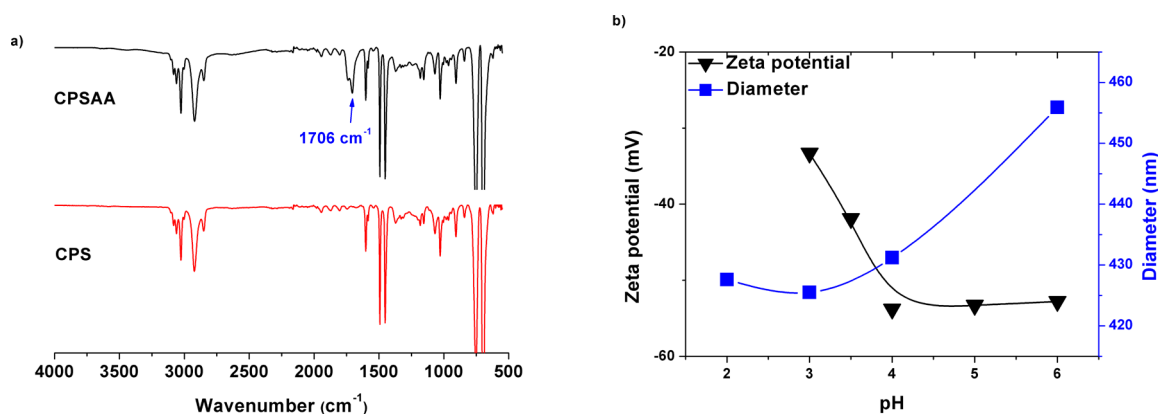

Figure 1. (a) Optical micrograph of positively charged large particles (PLPS). (b) The size distribution of PLPS determined from optical micrographs as shown in panel a. The distribution shows a diameter of 5 ± 1 μm. TEM images of negatively charged small particles (c) CPS (without acrylic acid) and (d) CPSAA (with acrylic acid as comonomer).

Figure 2. (a) Infrared spectra of CPSAA (top, black) and CPS (bottom, red). The highlighted signal at 1706 cm^{-1} is characteristic for the carbonyl stretching vibration of incorporated acrylic acid monomers. (b) Zeta potential (black triangles) and hydrodynamic diameter (blue squares) of CPSAA as a function of pH.

potential and the hydrodynamic diameter of CPSAA as a function of pH. As depicted in Figure 2b, the zeta potential increased from −53 to −33 mV by lowering pH from 6 to 3. The hydrodynamic diameter of CPSAA decreased from 455 to 425 nm by tuning pH from 6 to 2. The clear dependence of the zeta potential and the hydrodynamic diameter on pH find their origin in the pH-responsive properties of the PAA-rich outer shell on the CPSAA colloids. The pK_a of AA is 4.25 without interaction with other carboxyl groups in water,[27] at pH = 6, the charge density of the colloids is large due to the deprotonation of the carboxylic acids of the incorporated acrylic acid comonomers. This increased charge density generates a more pronounced electrostatic repulsion between the PAA-rich segments, resulting in swelling of the particles. The observation that the hydrodynamic diameter keeps increasing, while the zeta potential is fairly constant in a pH range of 4 to 6 might be rationalized by counterion condensation.[27] While not fully understood at this point, we expect that the high surface density of chargeable groups causes counterion condensation, leading to a fairly constant surface potential as a function of pH in the pH range from 4 to 6. In contrast, pH has only negligible influence on the hydrodynamic diameter and zeta potential of CPS (see Figure S1). pH independent size and zeta potential were anticipated for these nonfunctionalized polystyrene particles because the surface-immobilized sulfate groups are not pH-responsive within this pH window (p$K_a \approx 2$).[28] Table 1 summarizes all physicochemical properties of the synthesized particles.

Table 1. Charged Surface Functionalities, Size, and Zeta Potentials of as Synthesized Particles PLPS, CPS, and CPSAA

particles	charged surface functionalities	diameter	zeta potential[c] [mV]
PLPS	−N$^+$(CH$_3$)$_3$	5 ± 1 μm[a]	55.7 ± 8.2
CPS	−OSO$_3^-$	470 ± 18 nm[b]	−61.7 ± 7.0
CPSAA	−OSO$_3^-$/ −COO$^-$	461 ± 11 nm[b]	−62.3 ± 7.1

[a]Obtained by analyzing 100 particles from optical micrographs. [b]Hydrodynamic diameter as determined with DLS, measured in Milli-Q H$_2$O. [c]Measured in Milli-Q H$_2$O.

3.2. Influence of Polyelectrolytes on Encapsulation Behavior in Water.

For all encapsulation experiments, the smaller, negatively charged colloids were added in large excess with respect to the larger positively charged spheres to achieve complete encapsulation (see Supporting Information S3 for the details). As a starting point we investigated the encapsulation behavior of the CPS/PLPS system. Figure 3a shows an optical micrograph of a typical aggregate obtained after mixing PLPS and CPS in pure water. As can be seen, only a small fraction of the PLPS surface was covered by CPS. The resulting surface coverage was approximately 6%. Details on calculations of these surface coverages can be found in the Supporting Information (Figure S2). The surface coverage can be increased by addition of salt. As shown in Figure S3a, the surface coverage reached approximately 20% when particles were mixed in 10 mM aqueous NaCl solution. The fact that the surface coverage increases by addition of salt implies that electrostatic repulsions between the adsorbed CPS play a role in the encapsulation process. However, in 10 mM aqueous NaCl solution, the Debye length is approximately 3 nm, while the surface
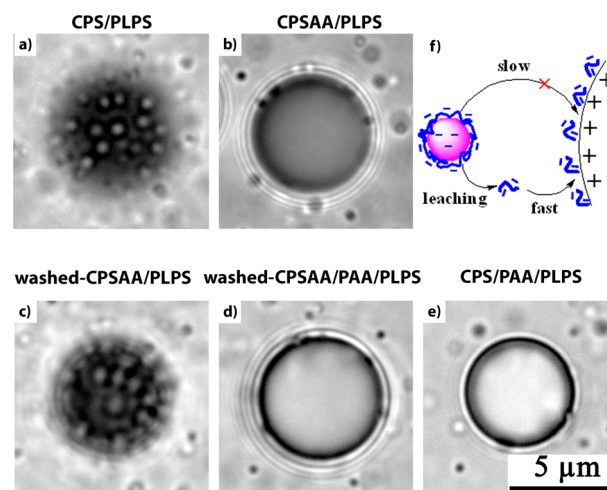
Figure 3. Representative optical micrographs of a mixed dispersion containing (a) CPS/PLPS, (b) CPSAA/PLPS, (c) washed-CPSAA/PLPS, (d) washed-CPSAA/PAA/PLPS, and (e) CPS/PAA/PLPS in pure H$_2$O. (f) Schematic illustration of the proposed mechanism in the CPSAA/PLPS system. Scale bar: 5 μm for all images.

separation between the adsorbed CPS is on the order of 100 nm. The remarkable large surface separation between the adsorbed CPS even with small Debye length excludes a direct effect of the electrostatic repulsions. As will be discussed later, the influence of the electrostatic repulsions on the surface coverage may be indirect via coupling with hydrodynamics.

Surprisingly, at least at first glance, a distinctly different clustering behavior was observed when PLPS were mixed with CPSAA. In pure water, CPSAA adsorbed to a significantly lesser degree onto PLPS than CPS (Figure 3a, b). This low coverage was measured regardless of the ionic strength of the continuous phase (Figure S3b). Because both particle species are oppositely charged, we expected to observe encapsulation efficiencies of the CPSAA/PLPS system comparable to those observed for the CPS/PLPS system. The fact that CPSAA hardly adsorb implies the existence of other factors that prevent efficient attachment of CPSAA onto PLPS.

One possible explanation is the steric repulsion caused by the diffusive PAA surface layer of the CPSAA particles. This steric effect was excluded by performing the heteroaggregation experiments of PLPS and PVP stabilized polystyrene particles (PS(PVP)), the results of which are comparable to those observed for the CPS/PLPS system (see Supporting Information S6 for the details).

In different types of cross-linked particles, it has been observed that cross-linking is incomplete resulting in a (small) fraction of polymers that remains unbound to the overall cross-linked network. Consequently, these noncross-linked polymers can migrate from the particle's interior into the continuous phase.[29] If we extend these findings to our systems, we might expect a (very) small fraction of PAA-rich polyelectrolytes to be leaching out from the CPSAA particles. On the basis of the monomer feeds used to synthesize CPSAA and PLPS, we can roughly estimate the minimal fraction of the initially incorporated acrylic acid moieties that should be expelled in order to neutralize the positive charges on PLPS. If we assume full monomer conversion, 1 g of CPSAA particles contains 10^{-3} mol AA, while 1 g of PLPS has 5.6 × 10^{-5} mol METMAC units. Combining these numbers with the volume fraction ratio of CPSAA to PLPS employed during the encapsulation

experiments (Table S1), leads to the conclusion that the negatively chargeable groups from incorporated AA are in an approximately 300 times excess compared to the positive METMAC-related charges. This calculation reveals that only 0.3% of PAA leaching from the CPSAA particles would be sufficient to neutralize the charges of PLPS. The fact that only a small fraction of free polymer is required to significantly alter the surface charge of PLPS makes this hypothesis plausible. Moreover, leaching of PAA-rich polyelectrolytes from CPSAA into the aqueous solution is favored by the hydrophilic nature of these polymers.

To experimentally verify if PAA-rich polyelectrolytes were being expelled from CPSAA, a CPSAA dispersion was centrifuged and the top half of the supernatant was carefully collected. PLPS were subsequently dispersed in the collected supernatant and its zeta potential was measured. To be consistent with respect to the encapsulation experiments, the volume fraction ratio of CPSAA to PLPS in this experiment is the same as the one used throughout all encapsulation experiments. The obtained zeta potential of PLPS dispersed in the supernatant was -35 ± 7.3 mV. Compared to its value of 55.7 ± 8.2 mV in pure water, the zeta potential clearly reversed, providing experimental evidence of PAA-rich polyelectrolytes leaching into the continuous phase. Evidently, the amount of expelled polymer is sufficient to reverse the charge of PLPS. The leaching of the PAA-rich polyelectrolytes was independently corroborated by measuring the IR spectrum of the dried supernatant. The obtained spectrum revealed the presence of signals at 1706 and 700 cm^{-1} corresponding to the C=O stretching vibration of the polymerized AA, and the aromatic C–H out-of-plane vibration of incorporated styrene monomers, respectively. These results clearly indicate that polyelectrolytes composed of AA and styrene monomers are present in the supernatant and have leached out of the colloidal particles (Figure S5). As the intensity of the C=O stretching vibration relative to the C–H vibration of styrene is significantly larger in the spectrum of the dried supernatant than it is in the spectrum of the particles CPSAA, we refer to the free polymer as "PAA-rich".

Given the fact that free polyelectrolytes are present in our mixed dispersions, we can speculate the effect this has on the heteroaggregation of the two particle species. Kinetically, the free PAA-rich polyelectrolytes are expected to attach onto PLPS faster than CPSAA. The exact molecular weight of expelled PAA-rich polyelectrolytes is unknown, but for a typical soap-free emulsion polymerization reaction, polymers with maximum molecular weights on the order of 10^5 g·mol^{-1} are formed.[30] The radii of gyration of these polymers are roughly 15 nm.[31] On the basis of the Stokes–Einstein equation this translates into diffusion coefficients that are at least an order of magnitude larger than those for CPSAA.[32] Naturally, adsorption of free PAA-rich polyelectrolytes leads to a decreased tendency for the CPSAA particles to aggregate with the partially charge neutralized or even charge reversed PLPS colloids (Figure 3f).

With these considerations and experimental evidence in hand, the following experiments were conducted to investigate the influence of free PAA on the encapsulation behavior in more detail. First, we thoroughly washed CPSAA to remove any unbound PAA-rich polyelectrolytes. After washing, we immediately performed the same encapsulation experiment as described before in order to avoid remaining noncross-linked PAA-rich polyelectrolytes to migrate from the particle's interior

to the aqueous phase. As shown in Figure 3c, after the additional washing steps, significantly more CPSAA particles attached onto PLPS compared to the unwashed particles (Figure 3b).

In the second experiment, we deliberately mixed PLPS and washed-CPSAA with commercial PAA. Before doing this, we mixed PLPS with solutions containing different concentrations of the commercial PAA and measured their zeta potentials. To be consistent with respect to the amount of leached PAA-rich polyelectrolytes in the CPSAA/PLPS system, the concentration of free PAA was chosen such that the resulting zeta potential of PLPS in this experiment (-33.6 ± 9 mV) closely matched the zeta potential previously measured after dispersing PLPS in the supernatant of CPSAA (-35 ± 7 mV). As shown in Figure 3d, the washed-CPSAA/PAA/PLPS system showed similar encapsulation behavior as that of the CPSAA/PLPS system, where an extremely low coverage was observed.

The final experiment was conducted by introducing the same amount of commercial PAA as that used in the second experiment into the CPS/PLPS system (the CPS/PAA/PLPS system, Figure 3e). Once more the introduction of PAA in the system resulted in similar encapsulation behavior as that observed for the CPSAA/PLPS system.

This set of experiments shows that the low coverage of the CPSAA/PLPS system obtained in pure water can be ascribed to the presence of free PAA-rich polyelectrolytes that leached from the CPSAA colloids. Interestingly, making use of this serendipitous observation, we are able to control the encapsulation behavior of oppositely charged colloids by simply adjusting the solution pH in the presence of polyelectrolytes. We elaborate on this in the next sections.

3.3. Influence of Polyelectrolytes on Encapsulation Behavior as a Function of pH.
As shown in the previous section, the competitive adsorption between leached PAA-rich polyelectrolytes and CPSAA results in extremely low coverage of CPSAA onto PLPS in pure water. Because PAA is pH-responsive, one would expect that at low pH, where the PAA chains are partially protonated, a fraction of the positive charges on PLPS will become accessible, promoting adsorption of CPSAA onto PLPS. In other words, the surface coverage of CPSAA on PLPS should be higher at lower pH. Note that CPSAA particles not only contain carboxyl groups but also approximately 2% sulfate groups relative to the number of carboxyl groups, according to the feed molar ratio between KPS and AA. The sulfate groups are still expected to be negatively charged at low pH, at least as long as pH $\geq$ p$K_{a,\text{sulfate group}}$. Therefore, at low pH, significant surface coverage is expected driven by the negatively charged sulfate groups on CPSAA and positively charged quaternary amine moieties on PLPS. To verify this hypothesis, we carried out encapsulation experiments in aqueous solutions with pH values ranging from 2 to 6. As shown in Figure 4, for pH < 4 (Figure 4a,b), relatively high surface coverages of approximately 30% were indeed observed. The maximum coverage of approximate 30% observed here is in agreement with those reported by Harley who used electron microscopy to analyze the surface coverage after heteroaggregation.[33] The relatively low value of the maximum coverage (i.e., only 30%) is ascribed to random sequential adsorption in combination with hydrodynamic interactions (see the Supporting Information S8 for details), although the detailed mechanism is not clear.[34,35] For pH values ranging from 4 to 6 (Figure 4c,d), microscopy analysis of the heteroaggregates revealed a low coverage (less than 5%). The trend in surface
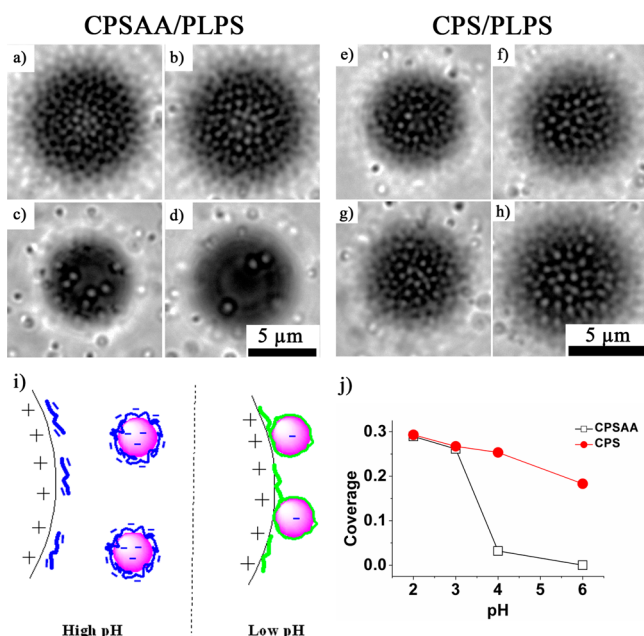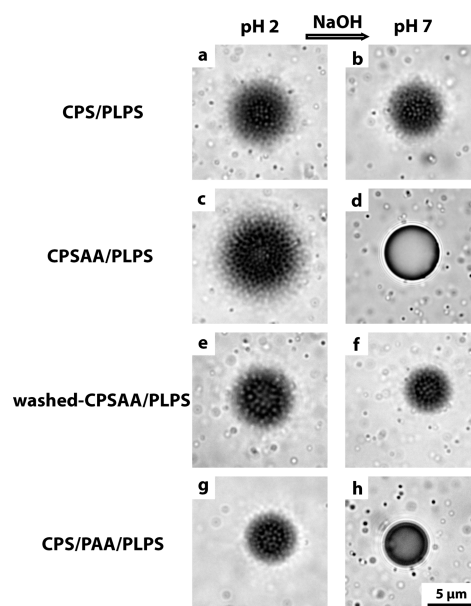
Figure 4. (a−h) Representative optical micrographs of coverage as a function of pH for the system of CPSAA/PLPS (left column) and CPS/PLPS (right column). pH = (a,e) 2, (b,f) 3, (c,g) 4, and (d,h) 6. (i) Schematic illustration for the encapsulation process of the CPSAA/PLPS system in dispersions of high and low pH values. Blue and green represent negatively charged PAA and protonated PAA, respectively. (j) Surface coverage as a function of pH for the system of CPSAA/PLPS (black open squares) and CPS/PLPS (red solid dots). Ionic strength = 10 mM. Scale bar: 5 µm for all images.


Figure 5. Optical micrographs of detachment results of (a,b) CPS/PLPS, (c,d) CPSAA/PLPS, (e,f) washed-CPSAA/PLPS, and (g,h) CPS/PAA/PLPS from pH 2 (a,c,e,g) to pH 7 (b,d,f,h) by addition of aqueous NaOH solution. Scale bar: 5 µm for all panels.

coverage within this pH range is in agreement with our expectations. As depicted in Figure 4i, at high pH (Figure 4i, left) the PAA-rich polyelectrolytes are highly charged and therefore capable of efficiently reversing the charge of the large particles, which prohibits CPSAA attachment. At low pH (Figure 4i, right), the PAA-rich polyelectrolytes are protonated, leading to the situation where sufficient positive charges on the large particles are accessible for CPSAA, resulting in relatively efficient encapsulation with a coverage of approximately 30%. In contrast, for the CPS/PLPS system without polyelectrolytes the encapsulation efficiency was found to be only weakly dependent on the solution pH (Figure 4).

From these experiments, we conclude that we can readily tune the surface coverage by adjusting the solution pH and that the aggregation process is largely governed by the charge density of the polyelectrolytes.

3.4. Reversible Encapsulation of CPSAA/PLPS. With experimental evidence that the degree of encapsulation is effectively determined by the charge density of the PAA-rich polyelectrolytes, we proceeded by investigating the influence of polyelectrolytes on the ability of small particles to detach from PLPS. For all the systems we investigated, high coverages of approximately 30% were observed at pH 2 (Figure 5). While increasing pH to 7 by the addition of aqueous NaOH solution, different degrees of detachment were observed depending on whether or not PAA had been present. pH 7 was chosen as the highest pH in our studies in order to prevent hydrolysis of the ester groups of METMAC, which would result in an irreversible charge reversal of PLPS (see Figure S6 for more information). In the CPS/PLPS (Figure 5b) and washed-CPSAA/PLPS system (Figure 5f), no detachment of small particles from PLPS

was observed. In contrast, the CPSAA/PLPS (Figure 5d) and CPS/PAA/PLPS systems (Figure 5h) showed that the majority of the small particles detached after an increase in pH, revealing the essential role of PAA in facilitating particles detachment. Furthermore, comparing the degrees of detachment observed for the CPSAA/PLPS and washed-CPSAA/PLPS systems, again confirms that it is the free PAA leached from CPSAA rather than the PAA chemically bound to CPSAA that dominates the detachment behavior (Figure 5 panel d for CPSAA/PLPS system and panel f for washed-CPSAA/PLPS system). Furthermore, we speculate that the free PAA acts as steric barrier restricting the minimal distance that CPSAA and PLPS can approach, resulting in a weaker van der Waals attraction, facilitating particle desorption even further.

With experimental evidence that the coverage is pH dependent and CPSAA are able to detach from PLPS by raising pH in the CPSAA/PLPS system, we accomplished a fully reversible and repeatable encapsulation of PLPS by CPSAA. We started at pH 2.5 instead of 2 because it yields a dispersion with a lower ionic strength and allows for more reversible encapsulation cycles. As shown in Figure 6a, CPSAA significantly covers the PLPS surface under this condition. When we raised pH to 7, most of the CPSAA particles desorbed from PLPS (Figure 6b). Encapsulation could be triggered again by lowering pH back to 2.5, as shown in Figure 6c. This reversible adsorption and desorption could be repeated 3 times up to the point where the ionic strength of the dispersing medium was too high, causing aggregation of both types of particles. The number of cycles could probably be increased by cycling between closer pH values. Furthermore, as already shown in Figure 5g,h, we expect the system of CPS/PAA/PLPS to show similar reversible encapsulation behavior. The aggregation is dominated by the free polyelectrolytes rather than by the chemical details of the participating species, making this approach a general strategy to control hetero-aggregation processes.
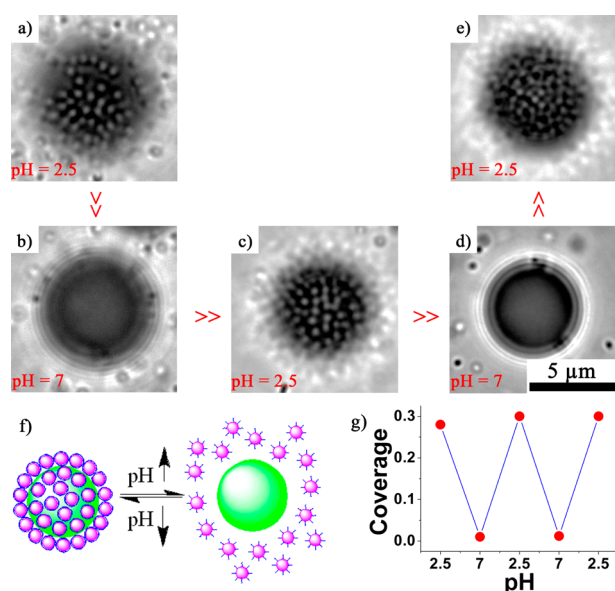
Figure 6. Reversible encapsulation of CPSAA/PLPS. (a–e) Optical micrographs of CPSAA/PLPS in pH = 2.5 and pH = 7 repeatedly; (f) Schematic illustration of reversible encapsulation behavior of CPSAA/PLPS. (g) Surface coverage by cycling pH for the CPSAA/PLPS system. Scale bar: 5 μm for all panels.

4. CONCLUSIONS

A colloidal model system capable of undergoing reversible encapsulation mediated by polyelectrolytes was developed. The system consists of positively charged large polystyrene microspheres and negatively charged smaller polystyrene particles that were decorated with a pH-responsive PAA outer layer. Reversible encapsulation was observed in the presence of small concentrations of unbound PAA polyelectrolytes in the continuous phase. At high pH, the PAA polyelectrolytes are highly charged and, therefore when adsorbed, able to reverse the charge of the large positively charged particles. Charging reversal causes an effective electrostatic repulsion between the two particle species, eventually resulting in low coverage of the large particles by the small particles. At low pH, the PAA polyelectrolytes are protonated. Under these conditions, positive charges on the large particles are accessible for the small oppositely charged particles, which leads to relatively high coverage. Furthermore, the presence of the PAA polyelectrolytes also allows small particles to desorb from large particles under appropriate change of pH. Finally, reversible encapsulation of large particles by small particles was achieved by cycling pH between 2.5 and 7 in the presence of polyelectrolytes.

Even under optimal conditions, a relatively low maximum coverage of approximately 30% was observed that is ascribed to a random sequential adsorption mechanism combined with hydrodynamic interactions.

We showed that polyelectrolytes can be used to control heteroaggregation of oppositely charged colloids. Moreover, the tunability of the coverage and reversibility of encapsulation of our system provide a potential platform to prepare sophisticated hierarchical assemblies, such as raspberry-like composites, colloidal molecules, and colloidal chains.[1,4,36]

■ ASSOCIATED CONTENT

ⓢ Supporting Information

The Supporting Information is available free of charge on the ACS Publications website at DOI: 10.1021/acs.langmuir.7b00845.

Movie of the heteroaggregation process between CPSAA and PLPS recorded with the optical microscope (AVI) Table of experimental conditions of encapsulation studies, plots of the zeta potential and the hydrodynamic diameter of CPS as a function of pH, theoretical calculation of the maximal number of small particles absorbing onto a larger central sphere, surface coverage calculation, optical micrographs of the heteroaggregates of CPS/PLPS and CPSAA/PLPS in 10 mM aqueous NaCl solution, optical micrographs of the heteroaggregates of PLPS/PS(PVP) in pure water and 10 mM aqueous NaCl solution, infrared spectra of pure poly-(acrylic acid) (PAA), the dried supernatant (PS−PAA) and CPSAA, discussion of relatively low maximum coverage, plots of the evolution of the zeta potential of PLPS at pH 3, 6 (pure water), 9, 10 and 11 (PDF)

■ AUTHOR INFORMATION

Corresponding Author
*E-mail: w.k.kegel@uu.nl.

ORCID ⓘ
Yong Guo: 0000-0002-5609-5550
Bas G. P. van Ravensteijn: 0000-0001-9024-3927

Present Address
†(B.G.P.v.R.) Department of Chemical Engineering, University of California Santa Barbara, Santa Barbara, CA 93105, USA.

Author Contributions
The manuscript was written through contributions from all authors. All authors have given approval to the final version of the manuscript.

Notes
The authors declare no competing financial interest.

■ REFERENCES

(1) Lan, Y.; Wu, Y.; Karas, A.; Scherman, O. A. Photoresponsive Hybrid Raspberry-Like Colloids Based on Cucurbit[8]uril Host−Guest Interactions. *Angew. Chem., Int. Ed.* **2014**, *53* (8), 2166−2169.

(2) Leunissen, M. E.; Christova, C. G.; Hynninen, A.-P.; Royall, C. P.; Campbell, A. I.; Imhof, A.; Dijkstra, M.; van Roij, R.; van Blaaderen, A. Ionic colloidal crystals of oppositely charged particles. *Nature* **2005**, *437* (7056), 235−240.

(3) Shevchenko, E. V.; Talapin, D. V.; Kotov, N. A.; O'Brien, S.; Murray, C. B. Structural diversity in binary nanoparticle superlattices. *Nature* **2006**, *439* (7072), 55−59.

(4) Snoswell, D. R. E.; Brill, R. K.; Vincent, B. pH-Responsive Microrods Produced by Electric-Field-Induced Aggregation of Colloidal Particles. *Adv. Mater.* **2007**, *19* (11), 1523−1527.

(5) Furusawa, K.; Anzai, C. Heterocoagulation behaviour of polymer latices with spherical silica. *Colloids Surf.* **1992**, *63* (1), 103−111.

(6) Suwabe, C.; Nagao, D.; Ishii, H.; Konno, M. Chemical bonding heterocoagulation of nanoparticles onto polymeric spheres by two-step addition of polymerizable coupling agent. *Colloid Polym. Sci.* **2015**, *293* (7), 2095−2100.

(7) Zhang, S.; Shao, Y.; Yin, G.; Lin, Y. Electrostatic Self-Assembly of a Pt-around-Au Nanocomposite with High Activity towards Formic Acid Oxidation. *Angew. Chem., Int. Ed.* **2010**, *49* (12), 2211−2214.

(8) Pan, Y.; Wang, J.; Wang, Y.; Wang, Z. PS Microspheres Coated by AuNPs via Thermodynamic Driving Heterocoagulation and Their High Catalytic Activity. *Macromol. Rapid Commun.* **2014**, *35* (6), 635−641.

(9) Li, M.; Chen, G.; Bhuyain, S. The induction phenomenon and catalytic deactivation of thiolate-stabilized raspberry-like polymer composites coated with gold nanoparticles. *Nanoscale* **2015**, *7* (6), 2641−2650.

(10) Ming, W.; Wu, D.; van Benthem, R.; de With, G. Super-hydrophobic Films from Raspberry-like Particles. *Nano Lett.* **2005**, *5* (11), 2298−2301.

(11) Carcouët, C. C. M. C.; Esteves, A. C. C.; Hendrix, M. M. R. M.; van Benthem, R. A. T. M.; de With, G. Fine-Tuning of Super-hydrophobicity Based on Monolayers of Well-defined Raspberry Nanoparticles with Variable Dual-roughness Size and Ratio. *Adv. Funct. Mater.* **2014**, *24* (36), 5745−5752.

(12) Li, Y.; Pan, Y.; Zhu, L.; Wang, Z.; Su, D.; Xue, G. Facile and Controlled Fabrication of Functional Gold Nanoparticle-coated Polystyrene Composite Particle. *Macromol. Rapid Commun.* **2011**, *32* (21), 1741−1747.

(13) Chao, Z.; Song, L.; Zhou, Y.; Nie, W.; Chen, P. Impact of PS/SiO2 morphologies on the SERS activity of PS/SiO2/Ag nanocomposite particles. *Colloid Polym. Sci.* **2014**, *292* (11), 2841−2848.

(14) Li, G.; Yang, X.; Wang, J. Raspberry-like polymer composite particles via electrostatic heterocoagulation. *Colloids Surf., A* **2008**, *322* (1−3), 192−198.

(15) Kanahara, M.; Shimomura, M.; Yabu, H. Fabrication of gold nanoparticle-polymer composite particles with raspberry, core-shell and amorphous morphologies at room temperature via electrostatic interactions and diffusion. *Soft Matter* **2014**, *10* (2), 275−280.

(16) Liu, B.; Zhou, M.; Liu, H.; Wang, X.; Yang, X. Binary colloidal hetero-coagulation for raspberry-like particles through azide−alkyne click reaction. *Colloids Surf., A* **2013**, *436*, 1027−1033.

(17) Wu, Q.; Wang, Z.; Kong, X.; Gu, X.; Xue, G. A Facile Strategy for Controlling the Self-Assembly of Nanocomposite Particles Based on Colloidal Steric Stabilization Theory. *Langmuir* **2008**, *24* (15), 7778−7784.

(18) Song, T.; Liu, T.; Yang, X.; Bai, F. Raspberry-like particles via the heterocoagulated reaction between reactive epoxy and amino groups. *Colloids Surf., A* **2015**, *469*, 60−65.

(19) Garmann, R. F.; Comas-Garcia, M.; Knobler, C. M.; Gelbart, W. M. Physical Principles in the Self-Assembly of a Simple Spherical Virus. *Acc. Chem. Res.* **2016**, *49* (1), 48−55.

(20) Garmann, R. F.; Comas-Garcia, M.; Gopal, A.; Knobler, C. M.; Gelbart, W. M. The Assembly Pathway of an Icosahedral Single-Stranded RNA Virus Depends on the Strength of Inter-Subunit Attractions. *J. Mol. Biol.* **2014**, *426* (5), 1050−1060.

(21) Zlotnick, A.; Aldrich, R.; Johnson, J. M.; Ceres, P.; Young, M. J. Mechanism of Capsid Assembly for an Icosahedral Plant Virus. *Virology* **2000**, *277* (2), 450−456.

(22) Roos, W. H.; Bruinsma, R.; Wuite, G. J. L. Physical virology. *Nat. Phys.* **2010**, *6* (10), 733−743.

(23) Zhang, F.; Bai, Y.; Ma, Y.; Yang, W. Preparing of monodisperse and cation-charged polystyrene particles stabilized with polymerizable quarternary ammonium by dispersion polymerization in a methanol−water medium. *J. Colloid Interface Sci.* **2009**, *334* (1), 13−21.

(24) Liu, Q.; Li, Y.; Shen, S.; Zhou, Z.; Ou, B.; Tang, S. Preparation of Monodisperse Cationic Microspheres by Dispersion Polymerization of Styrene and a Cation-Charged Monomer in the Absence of a Stabilizer. *J. Macromol. Sci., Part A: Pure Appl.Chem.* **2011**, *48* (7), 518−525.

(25) Wang, P. H.; Pan, C. Y. Preparation of styrene/acrylic acid copolymer microspheres: polymerization mechanism and carboxyl group distribution. *Colloid Polym. Sci.* **2002**, *280* (2), 152−159.

(26) Hunter, R. J. *Zeta Potential in Colloid Science*; Academic Press, 1981.

(27) Ohshima, H. Electrophoretic Mobility of a Spherical Colloidal Particle in a Salt-Free Medium. *J. Colloid Interface Sci.* **2002**, *248* (2), 499−503.

(28) Haynes, W. M. *CRC Handbook of Chemistry and Physics*, 97th ed.; CRC Press, 2016.

(29) Dullens, R. P. A.; Claesson, E. M.; Kegel, W. K. Preparation and Properties of Cross-Linked Fluorescent Poly(methyl methacrylate) Latex Colloids. *Langmuir* **2004**, *20* (3), 658−664.

(30) Goodall, A. R.; Wilkinson, M. C.; Hearn, J. Mechanism of emulsion polymerization of styrene in soap-free systems. *J. Polym. Sci., Polym. Chem. Ed.* **1977**, *15* (9), 2193−2218.

(31) Reith, D.; Müller, B.; Müller-Plathe, F.; Wiegand, S. How does the chain extension of poly(acrylic acid) scale in aqueous solution? A combined study with light scattering and computer simulation. *J. Chem. Phys.* **2002**, *116* (20), 9100−9106.

(32) Levine, I. N. *Physical chemistry*, 5th ed.; McGraw-Hill, 2002.

(33) Harley, S.; Thompson, D. W.; Vincent, B. The adsorption of small particles onto larger particles of opposite charge Direct electron microscope studies. *Colloids Surf.* **1992**, *62* (1−2), 163−176.

(34) Feder, J. Random sequential adsorption. *J. Theor. Biol.* **1980**, *87* (2), 237−254.

(35) Ko, C.-H.; Bhattacharjee, S.; Elimelech, M. Coupled Influence of Colloidal and Hydrodynamic Interactions on the RSA Dynamic Blocking Function for Particle Deposition onto Packed Spherical Collectors. *J. Colloid Interface Sci.* **2000**, *229* (2), 554−567.

(36) Kraft, D. J.; Vlug, W. S.; van Kats, C. M.; van Blaaderen, A.; Imhof, A.; Kegel, W. K. Self-Assembly of Colloids with Liquid Protrusions. *J. Am. Chem. Soc.* **2009**, *131* (3), 1182−1186.